Morphological And Anatomical Variations Of The Infraorbital Canal And Infraorbital Foramen Using Cone-Beam Computed Tomography

Mir mahdi Seyedashrafi [1] , Maruf Noruzi Gangachin[2] , Mohamad Hossein Razeghinejad[3] , Taymaz MounesiRad* , Mahdi Sharifitabar

[1] Assistant professor, Department of oral and maxillofacial surgery, Dental Faculty, Urmia university of Medical Science, Urmia, Iran

[2] Assistant professor, Department of oral and maxillofacial radiology, Dental Faculty, Urmia University of Medical Science, Urmia, Iran

[3] Assistant professor, Department of Orthodontics, Dental Faculty, Urmia University of Medical Science, Urmia, Iran

4. Assistant professor, Department of Prosthodontics, Dental Faculty, Urmia University of Medical Science, Urmia, Iran

[5] Dentist, Dental Faculty, Urmia University of Medical Science, Urmia, Iran

*Correspond author: Taymaz MounesiRad

Department of Prosthodontics, School of Dentistry, Urmia University of Medical Sciences, Valfajr Blvd, Alborz street, Urmia, Iran.
DOI: 10.47750/pnr.2022.13.S07.965

Abstract

Objectives: This study aimed to assess the morphological and anatomical variations of the infraorbital canal/groove (IOC/G) complex and infraorbital foramen (IOF) using cone-beam computed tomography (CBCT).

Materials and Methods: A total of 300 adult patients had bilateral CBCT scans evaluated in this retrospective cross-sectional study. The frequency of different morphologies and lengths of the IOC/G, the shape of the IOF, the prevalence of accessory IOF (AIOF), the distance from the IOF to the inferior orbital rim (IOR) and lateral nasal wall (LNW), and the relationship of the IOC/G with the maxillary sinus based on gender and laterality were recorded. Data were analyzed using SPSS version 22 at a 0.05 level of significance.

Results: The frequency of "canal only" morphology in the IOC/G (60.5%) was higher than that of "canal and groove" (39.5%). The mean IOC/G complex length was 30.09±4.23 mm. The frequency of oval IOF (76.7%) was higher than that of round IOF (23.3%) and AIOF was found in 53.33% of cases. The mean IOF – IOR and IOF – LNW distances were 10.15±1.8 mm and 10.79±2.32 respectively. The IOC/G had severe protrusion into the maxillary sinus in 11.8% of the cases. Gender had a significant correlation with the canal length, anatomical shape of the IOF, presence of the AIOF, and distance from the LNW. Laterality had a significant correlation with the IOF shape ($P<0.05$).

Conclusion: This study suggests a new strategy for measuring the infraorbital canal and groove length separately for better evaluation of the infraorbital complex in further investigations and assessed the prevalence of infraorbital canal presence in the zygomatic recess of the maxillary sinus using CBCT images for the first time. Precise knowledge of IOC/G and IOF anatomic variation can help to modify the surgical approach and prevent postsurgical complications.

Keywords: cone-beam computed tomography; infraorbital foramen; infraorbital canal; infraorbital groove

INTRODUCTION

The infraorbital canal/groove (IOC/G) complex located in the inferior orbital rim (IOR) may be present in one of the three forms: groove only, canal only, or a combination of these two (1). It provides a passage for important anatomical structures, namely the infraorbital artery, vein, and nerve, through the infraorbital foramen (IOF) towards the anterior mid-face (2, 3). The position and anatomical variations of this complex are important determinants of the direction of incisions to be made in the floor of the orbit, sinus endoscopic surgeries, and IOR reconstruction (4) . It is believed that IOC/G is one of the weakest points of the orbital floor and therefore the most susceptible part of the infraorbital margin to fracture (5, 6) . Due to the insufficient protection of anatomical structures in this area, the risk of damage to these structures during fractures or reconstructive surgeries is very high. The rate of infraorbital nerve damage in maxillary fractures is reportedly 30% to 80% (4). Knowledge about the anatomy of the IOF and its accessory foramina and the exact position of the infraorbital artery is highly important in otorhinolaryngology, ophthalmology, dentistry, maxillofacial surgery, plastic surgical procedures of the mid-face and nasal alae, facial rejuvenation procedures, and augmentation of the nasolabial fold (7-10).

Assessment of the anatomy of the IOF and IOC/G on dry skulls or cadavers has some limitations, such as the inability to assess the intracanal anatomy from different aspects, and difficult linear and angular measurements (11). Three-dimensional (3D) radiographic assessment using computed tomography (CT) and cone-beam computed tomography (CBCT) has obviated such

limitations (12-14). An important advantage of 3D radiographic modalities for such assessments is that the age and gender of patients are known; the acquisition of such precise information about patients could make studies more systematic and accurate (8).

With the advances in surgical techniques for procedures in the antrum and orbital areas, a complete preoperative radiographic assessment of the IOC/G complex is imperative to minimize the rate of complications during the interventional procedures (15, 16). Even though CT is known as the best imaging modality for assessment of the paranasal sinuses and their adjacent structures, cross-sectional CBCT imaging is also optimal for imaging the bony structures of the maxillofacial region due to its lower patient radiation dose and higher sensitivity for detection and diagnosis of fine bony structures (17-20) .

Considering the presence of anatomical variations in different populations and races (21) , this study aimed to assess the morphological and anatomical variations of the IOF and IOC/G using CBCT.

Materials and Methods

This descriptive, retrospective, cross-sectional study was conducted with approval from the Intuitional Ethics Committee of Urmia University of Medical Science, West Azerbaijan, Iran. Medical record data (limited to maxillofacial CBCT images between February 2019 and August 2020) that had been obtained for purposes not related to this study, such as implant placement, assessment of the paranasal sinuses, and evaluation of anatomical structures of the midface, were collected.

The inclusion criteria were age over 18 years, complete and clear visualization of the IOC/G and maxillary sinuses on both sides of the scans, and absence of technical errors. The exclusion criteria were the presence of lesions in the IOC/G complex, a previous history of sinus surgery, the presence of pathological lesions, a midface fracture, changes caused by the presence of radiopaque objects in the jaw such as dental implants, and the presence of anomalies in the paranasal sinuses. A flowchart of the study design and evaluation is provided in Figure 1. Finally, 600 IOC/G complex images of 300 patients were evaluated by two observers.

Scanning Methods

The CBCT scans were obtained using a Promax 3D CBCT scanner (Planmeca, Helsinki, Finland) with a voxel size of 0.2 mm and a field of view of 11*14 cm .The exposure settings parameters were as follows: 90-kV tube voltage, 8–10 MA tube current (depending on patient body habitus), and 13.5-second exposure time. The scanned images were conveyed to the computer, and Promax 3D CT's built-in image analysis Romexis 5.1.1 software (PLANMECA) was used to make a 3-dimensional reconstruction of the scanned areas. The images were saved in DICM format

Image Evaluation Methods

The IOC/G and IOF were evaluated bilaterally using axial, coronal, and sagittal sections with a slice thickness of 0.2 mm and a slice interval of 1 mm. Before taking measurements, the images were adjusted according to specific landmarks (e.g., the nasal septum, the nasal floor) to obtain a reproducible position IOC or IOF. The parasagittal plane was positioned by moving the plane from the anterior nasal spine/nasal septum to a level at which the entire course of the IOC or IOF vertical diameter could be completely determined. The coronal plane was chosen at the level where the IOC protruded the most into the maxillary sinus, or the IOF horizontal diameter was opened in the anterior of maxilla. The axial plane was positioned parallel to the nasal floor/hard palate and passed through the IOC or IOF. The section best illustrating the interesting anatomy was selected for further evaluation.

IOC/G evaluation

The anatomy of the IOC/G was determined using the classification proposed by Scarfe (3) according to the visible degree of the bony roof of the canal covering the anterior portion of the complex on the sagittal plane as one of the following three variations: (I) canal only (Figure 2A), (II) groove only, and (III) groove and canal (Figure 2B)

The length of the IOC/G was determined by considering the path as a segmented curve using the methodology described by Przygocka et al. (6) and Fontoliete et al. (7).The distance between the lower anterior margin of the IOF and the posterior margin of the IOC covered by the bone of the orbital floor was considered the canal length. The distance between the anterior margin of the IOG (the posterior limit of the canal where there is no bony roof) and the posterior margin of the IOG (a site where the IOG is opposite the orbital face of the greater wing of the sphenoid bone) was measured as the groove length. Finally, the complex length was measured as the sum of the lengths of the IOC with and without the IOG for each variation (Figure 2C).

In cross-sectional planes, the relationship of the IOC/G with the maxillary sinus roof was evaluated and categorized as one of the following four types (5):

Type I: The IOC/G is completely within the bony roof of the maxillary sinus.

Type 2: Mild protrusion of the IOC/G with part of it protruding into the maxillary sinus.

Type 3: Severe protrusion of the IOC/G and its complete presence within the maxillary sinus.

Type 4: The IOC/G is located at the outer limit of the zygomatic recess of the maxillary bone (Figure 3).

IOF evaluation

In the coronal and sagittal planes, the distance at the opening of the foramen was measured as the horizontal and vertical diameters of IOF, respectively (Figure 3A, B). To determine the anatomical shape of the IOF, the difference between the two diameters and the mean of the two diameters were compared. If both values were the same, it was considered to have a round shape. If the horizontal diameter was larger, it was considered to have a horizontal oval shape, and if the vertical diameter was larger, it was considered to have a vertical oval shape.

The presence or absence of accessory IOF (AIOF) was also evaluated in the coronal, axial, and sagittal planes. Also, the notha sutura anterior to the anterior lacrimal crest [20] was precisely evaluated for the presence of accessory foramina concerning the IOC.

In the coronal section, the length of a vertical line parallel to the sagittal plane from the center of IOF to the superior point of the infraorbital margin was measured as IOF –IOR distance (Figure 3C).

In the coronal section, the length of a horizontal line parallel to the axial plane passing from the center of the IOF connected to the interaction point with the external border of the lateral nasal cavity bone was measured as the IOF-LNW distance (Figure 3D) [21].

Two independent observers (one oral and maxillofacial radiologist and one oral and maxillofacial surgeon) who were experts in the interpretation of CBCT scans evaluated the images. At the onset of the study, to standardize image interpretation, the two observers had a meeting and were completely educated about obtaining reproducible position of interest anatomy images and exact anatomic point localization for measurement. In a dimly lit room, the images were interpreted using a 15-inch liquid crystal display monitor (Toshiba satellite L40, Tokyo, Japan) with a resolution of 1367×768 pixels. The observers were allowed to adjust the brightness, contrast, and magnification of the images to obtain the best visual result.

All the measurements were performed once by the two observers on the same computer, and the average value was calculated for each measurement. After all of the data had been evaluated by both observers, a consensus meeting on debatable images was held. If no consensus could be reached, the decision of a third expert (an orthodontist) was accepted.

To assess intra-examiner reproducibility, 20% of randomly (http://www.random.org) selected images were evaluated by both observers four weeks after completion of the first evaluation.

Statistical Analysis

The collected data were analyzed using SPSS version 22. The min, max, mean, and SD values were calculated for the quantitative variables. The Kolmogorov-Smirnov test was used to assess the normal distribution of data. Accordingly, the non-parametric Mann-Whitney test and the parametric independent t-test were applied to analyze the data based on gender and laterality. The significance level was set at $P = 0.05$.

Inter-observer and intra-observer agreement were calculated using Cohen's kappa values. A kappa value below 0.40 was indicative of poor agreement, a kappa value of 0.40 to 0.75 indicated intermediate to good agreement, and a kappa value greater than 0.75 was indicative of excellent agreement beyond chance.

Results

The CBCT scans of 300 patients, including 131 males and 169 females, were evaluated; a total of 600 IOC/G complexes (300 on the right and 300 on the left) were assessed by two observers. Intra-examiner and inter-examiner reliability were 89% and 96%, respectively.

Table 1 presents the frequency distribution of the three morphological variants of the IOC/G, namely “canal only”, “canal and groove”, and “groove only”, as well as the mean and standard deviation of groove length and canal length in each variant based on gender and laterality. In total, the frequency of the “canal only” variant (60.5%) was higher than that of the “canal and groove” variant (39.5%). No case of “groove only” was found. The mean length of the complex was 30.09±4.23 mm. In cases with the “canal and groove” variant, the mean length of the IOG was 9.04±5.4 mm, while the mean length of the IOC was 21.73±5.8 mm. In cases with the “canal only” variant, the mean canal length was the same as the overall length of the complex, which was 29.56±3.05 mm. The IOC/G length was not significantly different between cases with “canal and groove” and “canal

only" variants (P>0.05). Statistical analysis of the data by the Mann-Whitney test revealed that canal length had a significant correlation with gender (P=0.008). No significant difference was noted between the right and left sides of the face or between males and females in any other variable (P>0.05).

Table 2 presents the relationship of the IOC/G with the maxillary sinus roof and its distribution based on gender and laterality. Mild protrusion (type II) was noted in 34.17% of the cases and severe protrusion (type III) was seen in 11.83% of the cases. In 3.01% of the cases, the IOC/G was located in the lateral wall of the maxillary sinus; however, the difference in its incidence was not significant between males and females or between the two sides of the face (P>0.05).

Table 3 presents the mean and standard deviation of the vertical and horizontal diameters of the IOF based on gender and laterality. The mean horizontal diameter of the foramen (3.54±0.54 mm) was greater than its mean vertical diameter (3.41±0.61). Males had significantly longer mean lengths of both horizontal and vertical diameters than females (P <0.05). A comparison of the dimensions of the IOF on the two sides revealed that the vertical diameter of the canal had a significant correlation with laterality (P=0.039) but the horizontal diameter of the canal had no significant correlation with laterality (P=0.75).

Table 4 presents the prevalence and frequency distribution of different shapes of the IOF based on gender and laterality. The frequency of oval IOF (51.67% horizontal oval and 25.01% vertical oval) was significantly higher than that of round IOF (23.32%). The anatomical shape of the canal had a significant correlation with gender (P=0.027) and laterality (P=0.034).

Table 5 presents the prevalence of AIOF and its distribution based on gender and laterality. AIOF was present in 53.33% of the cases, and its presence had a significant correlation with gender (P=0.007). However, it had no significant correlation with laterality (P=0.102).

Table 6 shows the mean and standard deviation of the distance from the IOF to the IOR and LNW based on gender and laterality. The mean distance from the IOF to the IOR was 10.15±1.8 mm. The distance between the IOF and IOR was slightly greater in males than females. However, the difference in this respect was not significant between males and females (P=0.508) or between the two sides of the face (P=0.982). The distance between the IOF and LNW in males was significantly greater than that in females (P=0.001); however, the difference in this respect was not significant between the two sides of the face (P=0.88).

Discussion

The anatomical position of the IOC/G complex is an important factor in determining the direction of surgical incisions to be made on the floor of the orbit. Although the infraorbital nerve and the vasculature are protected by the canal, they can be easily traumatized and damaged by manipulation of this region (3, 20). Scarfe et al. (3) were the first to describe the term "IOC/G complex" and defined three variants of "canal only," "groove only," and "canal and groove" according to the visible degree of the bony canal roof on panoramic images. In the same study, they evaluated 246 panoramic radiographs and reported that the IOC/G was visible on 81.3% of the images; the aforementioned three variants had a frequency of 42%, 13.25%, and 44.75%, respectively (3). The "canal only" variant was reported in the Chinese skulls, Egyptian skulls, and Turkish cadavers at 3.8%, 25%, and 50%, respectively (14, 23, 25) . The "canal and groove" variant was reported in 50% of the Turkish cadavers (14) . In the present study, the prevalence of "canal only"and "groove and canal" variants were 60.5% and 39.5%, respectively, and no case of "groove only" was found.

In the majority of anthropometric studies, the length of the bony roof of the canal covering the anterior portion of the complex is measured to describe the position of the canal and groove about the IOC/G complex (6, 14, 23). The canal and groove lengths reported in such studies ranged from 12.75 to 23 mm and 6 to 16 mm, respectively (5). Studies using CT and CBCT have reported different numerical values for the canal and groove lengths; however, the numerical values reported for the overall length of the complex are almost the same (12) . Variations in the reported range of values for the canal and groove length can be attributed to several reasons: The first reason is the variations in the definitions of groove and canal in different studies. Hwang et al. (8) did not consider the bony roof of the canal; instead, they discussed that the canal changes to a groove where it rotates from its superior-lateral path and becomes parallel to the floor of the orbit. In their study, the canal length and the groove length were reported to be 9.1±7.11 mm and 7.16±4.2 mm, respectively (8).Orhan et al. (25) used the same method and calculated the canal length as the distance between the IOF and the point of rotation of the canal axis. They measured the groove length as the sum of the length of the groove (without the bony canal roof) plus the length of the part of the canal parallel to the floor of the orbit that was covered with a bony roof. In the study by Orhan et al. (25), the canal length was 3.52±0.97 mm on the right side and 3.46±0.79 mm on the left side. In some of the anthropometric studies, the distance between the inferior border of the IOF and the limit of the bony roof of the canal was considered the IOC length, and the length of the segment without the

bony roof of the canal was considered the groove length (6).The second reason is the need to note the internal angulation of the canal Acar et al. (5) defined the internal angulation of the canal as the site of rotation of the canal from its original path. They stated that in the case of the presence of internal angulation, the canal length should be measured in two separate segments (5). Fontolliet et al. (7) used the segmentation technique to overcome this problem and reported the canal length, groove length, and complex length to be 24.9±2.09 mm, 4.6±1.7 mm, and 29±3.0 mm, respectively. The present study also used the segmentation technique to measure the length of the canal and groove and reported results similar to those of Fontolliet et al. (7). The third reason for the wide variation in the range of reported values for the canal and groove length in different studies that the studies do not differentiate between the canal length and groove length in their complete or partial forms, instead combining these two forms. The authors suggest that before measuring the canal and groove length, first, the morphology of the IOC/G should be identified according to the classification proposed by Scarfe et al. (3), and then the groove and canal length should be calculated separately for each variant. By doing so, the numerical value of the length can be more accurately calculated with a smaller standard deviation, and the canal and groove lengths of different variants could be compared with each other and with the values reported in other studies. The present study was the only radiographic study that calculated the canal and groove length separately for each IOC/G complex variant. Moreover, in the assessment of the canal length based on CT scans versus CBCT scans, it should be noted that the bony roof covering the posterior part of the canal is composed of very thin bone, which may not be well detected on CT scans. Considering the high potential of CBCT in visualizing the fine bony details, the numerical values obtained based on CBCT scans are more accurate (18) .

The protrusion of the IOC/G into the maxillary sinus is a common variation. The increased protrusion can increase the risk of canal dehiscence or thinness of the bony wall of the canal, and subsequently, the risk of iatrogenic injury to the canal contents. Different types of classifications and consequently different numerical values have been reported for the prevalence of protrusion of the IOC/G into the maxillary sinus (7, 18, and 26). However, the class representing complete protrusion of the IOC/G into the maxillary sinus is more important and has higher sensitivity during surgical procedures. Severe protrusion (type 3) of the IOC into the maxillary sinus had a prevalence ranging from 2.5% to 11.2% in the literature (5, 7, 18, 26-28) and 11.83% in the present study. Such a controversy in the reported values can be due to the use of different imaging modalities as well as racial differences. Most previous studies used type 1 to type 3 classifications for assessment of the protrusion of the IOC into the maxillary sinus (7, 18, 27, 28). Type 4 was first introduced by Rusu et al. (29)and its prevalence was reported by Gulay et al. (5) to be 8.5% in CT images. For the first time, the current study evaluated the prevalence of type 4 using CBCT images, and it was 3.01% in all cases. Surgeons may modify their surgical approach in cases in which this type of protrusion is identified by preoperative assessments (5).

Different studies have reported wide variations in the shape, dimensions, and exact position of the IOF in different populations and racial groups (6, 12). The anatomy of the IOF is determined by measuring the vertical and horizontal diameters of the foramen or assessing its anatomical shape (12). Most studies have reported greater vertical and horizontal diameters of the canal in males, compared with females (12). Hwang et al. (30)confirmed the hypothesis that the effect of artery diameter on canal dimensions is higher than the effect of nerve diameter. They theorized that the dimensions of the IOF are influenced by the climate discrepancies and that the diameter of the infraorbital artery is larger in cold climates; thus, the canal diameter in cold climates is larger than that in tropical areas (30). Martins-Ju´nior et al. (31) noticed a significant difference between the horizontal diameter on the right and left sides and discussed that the changes in the shape of the IOF must be related to the changes in the horizontal diameter of the canal. Different forms of the IOF, including its round, oval, semilunar, and D shapes, have been reported in the literature (12, 31, 32). In the current study, the frequency of oval IOF (76.7%) was higher than that of round shapes (23.3%). According to Orhan et al. (25) the anatomical shape of the IOF remains the same with age. In the study by Sokhn et al. (21) and Dagistan et al. (33), the IOF was round in 54.8% of the cases and oval or other shapes in the remaining cases. The presence of AIOF can increase the risk of accessory nerve damage (12, 30, 31). The frequency of AIOF ranges from 1.4% to 56.6% in the literature (29, 30) and it was found in 53.33% of cases in this study. In their review study, Hwang et al. (30) concluded that the frequency of AIOF varied significantly across continents, with an overall incidence of 16.9%8.6% in skulls and cadavers and being influenced by race and climate. Rusu et al. (29) evaluated the sutura notha anterior to the anterior lacrimal crest and concluded that AIOF was present unilaterally or bilaterally in this region in 6% of the cases (29). None of the previous studies had pointed to this topic. Such foramina in relation to the IOC can be well detected on CBCT scans (29). Variations in the frequency of AIOF can be due to variable methodology and racial differences. Also, considering the high prevalence of AIOF, care must be taken in determining the exact localization of the AIOF in different populations (7, 29, 30).

Different anatomical landmarks have been used for localization of the IOF when administering a nerve block; the most common is the IOF - IOR distance, which is used for extraoral block and radiofrequency neurotomy (12, 34). In the Caldwell-Luc surgical procedure, a flap is elevated to the level of the IOF, which causes paresthesia in 2- 9% of the cases; thus, the exact localization of the IOF is highly important (18). Leo et al. (35) discussed that the distance between the IOF and IOR remains constant after

20 years of age. This distance was reported to be 5-10.9 mm in a study on human skulls (25). The IOF-IOR distance in the 3D radiographic studies by Sokhn et al.(21) Hwang et al. (9) and Leo et al. (35), was reported to be 7.98±1.41 mm, 9.6±1.7 mm, and 8.42 mm respectively. The abovementioned values were lower than the corresponding values (10.15±1.8 mm) in our study. Such variations are probably related to racial differences between the study populations. Moreover, our study had a much larger sample size than all the aforementioned studies.

The IOF-LNW distance has also been evaluated using different imaging modalities such as lateral cephalometry, CT, and CBCT (12). This value was measured to be 14-18 mm on human skulls (5). The IOF-LNW distance was10.79±2.32 in the current study, which was close to the obtained values of the study by Sokhn et al.(21) and Bashi et al.(12) That report IOF-LNW distance 10.61±2.39 mm, 9.57±2.39 mm (right side), and 9.34±2.36 mm (left side), respectively.

Comparing the measurements based on patient sexuality, significantly greater values were found in males' canal length, anatomical shape of the IOF, presence of the AIOF, and distance from the LNW in the present study. Fontolliet et al. (7) found significant differences in the linear measurements related to the length of the IOC, IOC/G, and the IOF diameter in males. Orhan et al.(25) have shown significantly larger measurements for the IOC and IOG in male patients. Hwang et al.(8) found that the length of the IOG in males was significantly longer. Looking at differences related to the right and left sides of the measurements, laterality only had a significant correlation with the IOF shape in the present study. Fontolliet et al. (7) found no significant differences in the linear measurements related to laterality measurement.

Regarding the findings of the present study, this study possesses some limitations that have to be taken into consideration. This study reviewed a limited sample size from a single referral center in Urmia City. It needs a larger sample size from different cities in future studies to define the characteristics of the IOF in the Iranian population. These results certainly have to be interpreted with some caution, especially when comparing them across different populations. The choice of the reproducible positions of the planes and reference landmarks has its limitations due to the relatively small field of views of the CBCTs compared to CT scans. The sella turcica or the nasion can be used as stable reference structures.

Conclusion

This study suggests a new strategy for measuring the infraorbital canal and groove length separately for better evaluation of the infraorbital complex in further investigations and assessed the prevalence of infraorbital canal presence in the zygomatic recess of the maxillary sinus using CBCT images for the first time. Precise knowledge of IOC/G and IOF anatomic variation can help to modify the surgical approach and prevent postsurgical complications.

Conflicts of interest

There is no conflict of interest between the authors.

References

1. Attavar S. An Overview of the Antimicrobial Effect of Natural Irrigants in Disinfection of Root Canal System. Pharmacophore. 2022;13(1):79-82. https://doi.org/10.51847/PpJg04CzT9
2. Sharma N, De M, Pracy P. Recurrent facial paraesthesia secondary to maxillary antral cyst and dehiscent infraorbital canal: case report. The Journal of Laryngology and Otology. 2007;121:1.
3. Scarfe W, Langlais R, Ohba T, Kawamata A, Maselle I. Panoramic radiographic patterns of the infraorbital canal and anterior superior dental plexus. Dentomaxillofacial Radiology. 1998;27:85-92.
4. Bandyopadhyay T, Sapru B. Management of an isolated orbital blow-out fracture. Medical Journal, Armed Forces India. 200.60:392;4
5. Açar G, Özen KE, Güler İ, Büyükmumcu M. Computed tomography evaluation of the morphometry and variations of the infraorbital canal relating to endoscopic surgery☆. Brazilian journal of otorhinolaryngology. 2018;84:713-721.
6. Przygocka A, Szymański J, Jakubczyk E, Jędrzejewski K, Topol M, Polguj M. Variations in the topography of the infraorbital canal/groove complex: a proposal for classification and its potential usefulness in orbital floor surgery. Folia morphologica. 2013;72:311-317.
7. Fontolliet M, Bornstein MM, von Arx T. Characteristics and dimensions of the infraorbital canal: a radiographic analysis using cone beam computed tomography (CBCT). Surgical and radiologic anatomy. 2019;41:169-179.
8. Hwang SH, Kim SW, Park CS, Kim SW, Cho JH, Kang JM. Morphometric analysis of the infraorbital groove, canal, and foramen on three-dimensional reconstruction of computed tomography scans. Surgical and radiologic anatomy. 2013;35:565-571.
9. Hwang SH, Seo JH, Joo YH, Kim BG, Cho JH, Kang JM. An anatomic study using three-dimensional reconstruction for pterygopalatine fossa infiltration via the greater palatine canal. Clinical anatomy. 2011;24:576-582.
10. Suresh S, Patel AS, Dunham M, Heffner CL, Coté CJ. A randomized double-blind controlled trial of infraorbital nerve block versus intravenous morphine sulfate for children undergoing endoscopic sinus surgery: Are postoperative outcomes different. Anesthesiology. 2002;97:A1292.
11. Mavidis Kharalampos, Put V.A., Tarasenko S.V., Reshetov I.V. Comprehensive patient rehabilitation while performing immediate dental implant placement with the use of information-wave therapy (literature overview). J Adv Pharm Edu Res 2020;10(2):11-14.
12. Bahşi İ, Orhan M, Kervancıoğlu P, Yalçın ED. Morphometric evaluation and surgical implications of the infraorbital groove, canal and foramen on cone-beam computed tomography and a review of literature. Folia morphologica. 2019;78:331-343.
13. Gupta T. Localization of important facial foramina encountered in maxillo-facial surgery. Clinical anatomy. 2008;21:633-640.
14. Kazkayasi M, Ergin A, Ersoy M, Bengi O, Tekdemir I, Elhan A. Certain anatomical relations and the precise morphometry of the infraorbital foramen–

canal and groove: an anatomical and cephalometric study .The Laryngoscope. 2001;111:609-614.
15. Miracle A, Mukherji S. Conebeam CT of the head and neck, part 2: clinical applications. American Journal of Neuroradiology. 2009;30:1285-1292.
16. Polo CL, Abdelkarim AZ, von Arx T, Lozanoff S. The morphology of the infraorbital nerve and foramen in the presence of an accessory infraorbital foramen. Journal of craniofacial surgery. 2019;30:244-253.
17. Coulter VL, Holds JB, Anderson RL. Avoiding complications of orbital surgery: the orbital branches of the infraorbital artery. Ophthalmic Surgery, Lasers and Imaging Retina. 1990;21:141-143.
18. Haghnegahdar A, Khojastepour L, Naderi A. Evaluation of infraorbital canal in cone beam computed tomography of maxillary sinus. Journal of Dentistry. 2018;19:41.
19. Mozsary PG, Middleton RA. Microsurgical reconstruction of the infraorbital nerves. Journal of oral and maxillofacial surgery. 1983;41:697-700.
20. Zingg M, Chowdhury K, Lädrach K, Vuillemin T, Sutter F, Raveh J. Treatment of 813 zygoma-lateral orbital complex fractures: New aspects. Archives of Otolaryngology–Head & Neck Surgery. 1991;117:611-620.
21. Sokhn S, Challita R, Challita A, Challita R. The Infraorbital Foramen in a Sample of the Lebanese Population: A Radiographic Study. Cureus. 2019;11.
22. Hufschmidt K ,Bronsard N, Foissac R, Baqué P, Balaguer T, Chignon-Sicard B, et al. The infraorbital artery: clinical relevance in esthetic medicine and identification of danger zones of the midface. Journal of Plastic, Reconstructive & Aesthetic Surgery. 2019;72:131.136-
23. Chien H-F, Wu CH, Wen CY, Shieh JY. Cadaveric study of blood supply to the lower intraorbital fat: etiologic relevance to the complication of anaerobic cellulitis in orbital floor fracture. Journal of the Formosan Medical Association. 2001;100:19.197-2
24. Hindy A, Abdel-Raouf F. A study of infraorbital foramen, canal and nerve in adult Egyptians. Egyptian dental journal. 1993;39:573.
25. Orhan K, Misirli M, Aksoy S, Hincal USE, Ormeci T, Arslan A. Morphometric analysis of the infraorbital foramen, canal and groove using cone beam CT: considerations for creating artificial organs. The International Journal of Artificial Organs. 2016;39:28-36.
26. Yenigun A, Gun C, Uysal II, Nayman A. Radiological classification of the infraorbital canal and correlation with variants of neighboring structures. European Archives of Oto-Rhino-Laryngology. 2016;273:139-144.
27. Lantos J, Pearlman A, Gupta A, Chazen J, Zimmerman R, Shatzkes D, et al. Protrusion of the infraorbital nerve into the maxillary sinus on CT : prevalence, proposed grading method, and suggested clinical implications. American Journal of Neuroradiology. 2016;37:349-353.
28. Ference EH, Smith SS, Conley D, Chandra RK. Surgical anatomy and variations of the infraorbital nerve. The Laryngoscope. 20.1300-125:1296;15
29. Rusu M, Săndulescu M, Ilie O. Infraorbital canal bilaterally replaced by a lateroantral canal. Surgical and radiologic anatomy. 2015;37:1149-1153.
30. Hwang K, Lee SJ, Kim SY, Hwang SW. Frequency of existence, numbers, and location of the accessory infraorbital foramen. Journal of craniofacial surgery. 2015;26:274-276.
31. Martins-Júnior PA, Rodrigues CP, De Maria MLdA, Nogueira LM, da Silva JH, e Silva MRMA. Analysis of anatomical characteristics and morphometric aspects of infraorbital and accessory infraorbital foramina. Journal of craniofacial surgery. 2017;28:528-533.
32. Aggarwal A, Kaur H, Gupta T, Tubbs RS, Sahni D, Batra Y, et al. Anatomical study of the infraorbital foramen: a basis for successful infraorbital nerve block .Clinical anatomy. 2015;28:753-760.
33. Dağıstan S, Miloğlu Ö, Altun O, Umar E. Retrospective morphometric analysis of the infraorbital foramen with cone beam computed tomography. Nigerian Journal of Clinical Practice. 2017;20:1053-1064.
34. ,Nanayakkara DPeiris R, Mannapperuma N, Vadysinghe A. Morphometric analysis of the infraorbital foramen: the clinical relevance. Anatomy research international. 2016;2016.
35. Leo JT, Cassell MD, Bergman RA. Variation in human infraorbital nerve, canal and foramen. Annals of Anatomy-Anatomischer Anzeiger. 1995;177:93-95.

Figure legends

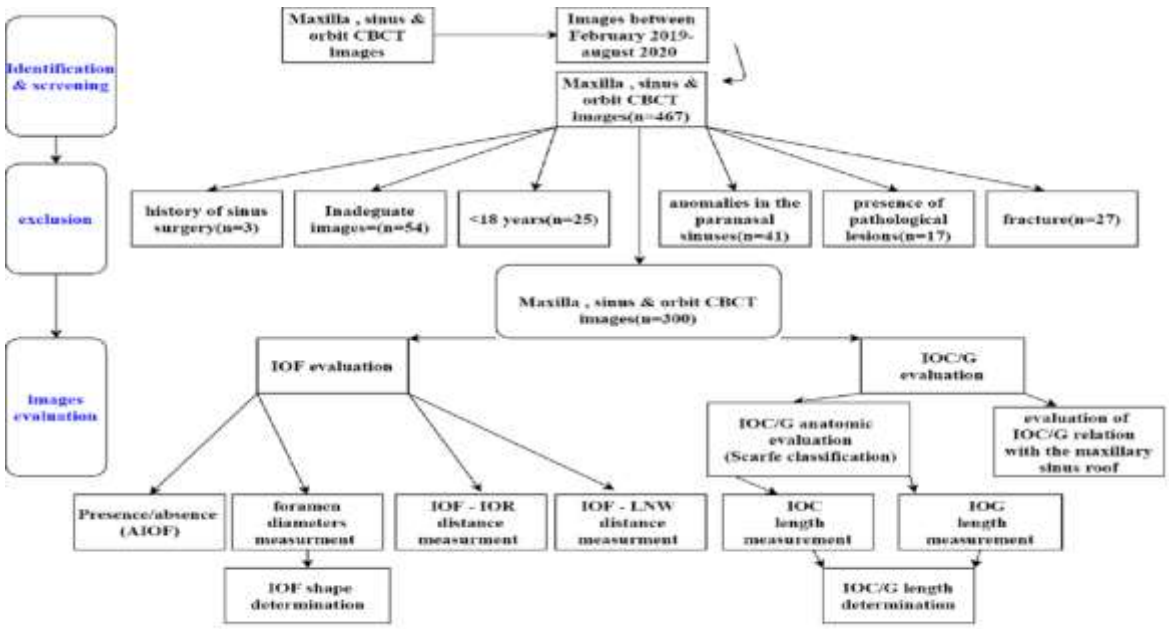

Figure 1. Flowchart of the study design and strategy

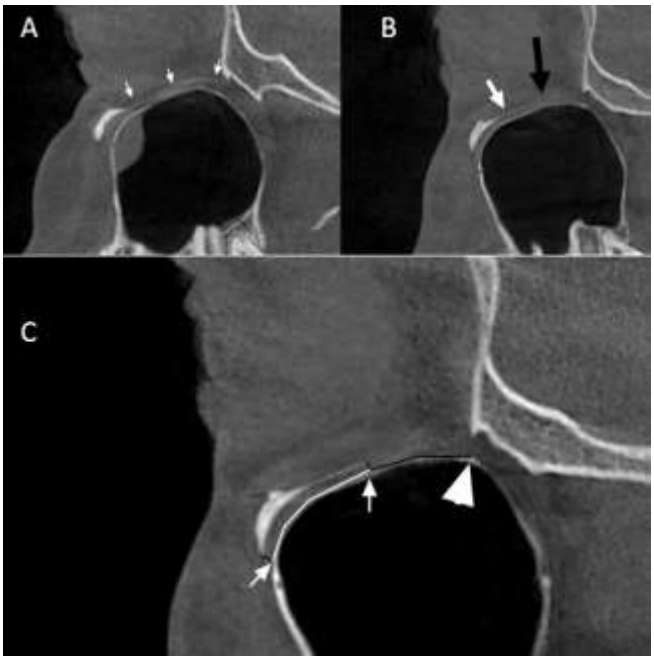

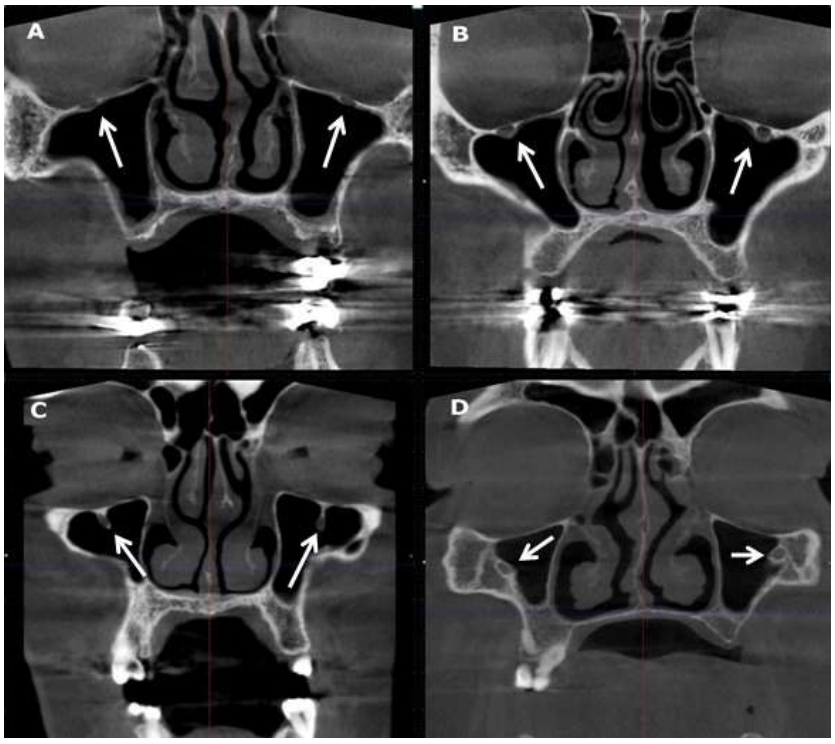

Figure 2. Assessment of the anatomical shape of the IOC/G according to the degree of visibility of the bony roof of the canal covering the anterior portion of the complex on sagittal plane :(A) Canal only ;(B) Groove (black arrow) and canal (white

arrow); (C) Linear measurements of the IOC length (the white line between two arrows) and IOG length (the black line between the middle arrow and arrowhead) on a segmented curve

Figure 3. Bilateral Coronal plane CBCT images depicting the relation of IOC/G to the maxillary sinus:

Type 1 (**A**) shows the IOC/G embedded in the maxillary sinus roof; type 2 (**B**) depicts the IOC/G partially protruding into the maxillary sinus; type 3 (**C**) shows the IOC/G entirely protruding into the maxillary sinus; type 4 (**D**) depicts The IOC/G is

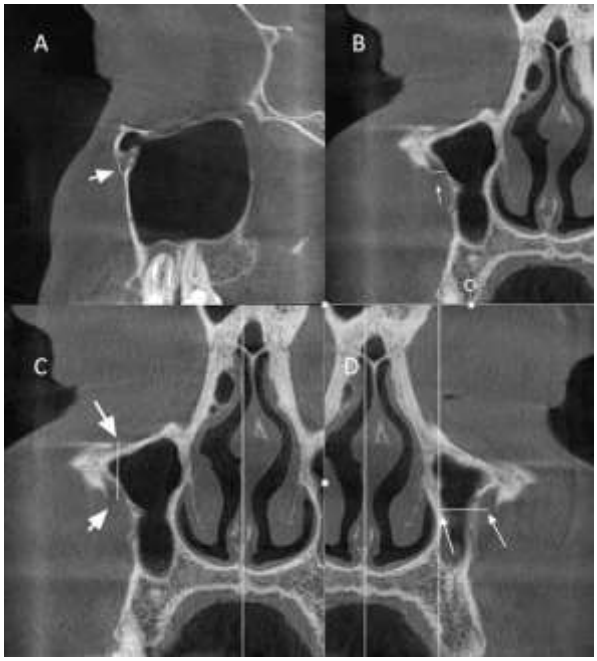

located at the outer limit of the zygomatic process of the maxillary bone

Figure 4. Linear measurements of the IOf were taken in CBCT images: distance of cortical border at the opening of the foramen was measured in the coronal plane as the horizontal diameter (A) and in the sagittal plane as vertical diameter (B); In the coronal section, IOF –IOR distance(c) was measured as the length of a vertical line (white line) parallel to the sagittal plane from the center of IOF (downer arrow) to the superior point of the infraorbital margin(upper arrow); the length of a horizontal line(white line) parallel to the axial plane and perpendicular to sagittal plane passes from the center of IOF(outer arrow) connected to the interaction point with the external border of lateral nasal cavity bone(inner arrow) was measured as IOF -LNW distance(D)

.